A Stochastic Rheological Model for the Calculation of Polymeric Fluids

Deepthika Senaratne
Department of Mathematics and Computer Science,
Fayetteville State University
1200 Murchison Road, Fayetteville, NC 28301, USA
Email: dsenaratne@uncfsu.edu

Abstract

A stochastic rheological model for the calculation of polymer stress in polymeric fluids is developed and evaluated. The model is microscopic-based and combines aspects of reptation, modified network and continuum models. A concentrated Polyisobutylene (PIB) solution is simulated for material functions in various rheometric flows. Comparisons made with available experimental data shows that the model predicts well the qualitative material behavior of the fluid in the rheometric flows considered. In most cases, the predictions agree quantitatively with the available experimental data.

Keywords: Polymeric Fluids, Stress Tensor, Rheological Models

1. Introduction

The total stress tensor $\boldsymbol{\sigma}$ for an incompressible fluid is given by

$$\boldsymbol{\sigma} = -p\boldsymbol{\delta} + \boldsymbol{\tau} \tag{1}$$

where p is an isotropic pressure, $\boldsymbol{\delta}$ is the second order unit tensor, and $\boldsymbol{\tau}$ is the extra-stress tensor. In the presence of a solvent, the extra stress tensor $\boldsymbol{\tau}$ can be written as

$$\boldsymbol{\tau} = \boldsymbol{\tau}_s + \boldsymbol{\tau}_p \tag{2}$$

where $\boldsymbol{\tau}_s$ is the solvent contribution, and $\boldsymbol{\tau}_p$ is the polymer contribution. In general, the solvent is Newtonian and the Newtonian stress contribution can be computed by $\boldsymbol{\tau}_s = \eta_s \left[\boldsymbol{\kappa} + \boldsymbol{\kappa}^{\dagger} \right]$ where $\boldsymbol{\tau}_s$ is the solvent viscosity, $\boldsymbol{\kappa}$ is the transpose of the velocity gradient tensor and $\dagger$ represents the

transpose. The polymer contribution τ_p has to be modeled with an appropriate rheological model which captures the correct visco-elastic behavior of the polymer. In this paper, we will focus on a microscopic-based stochastic model which combines the aspects of reptation and modified network models with continuum models.

In recent years, efficient stochastic simulation techniques have been derived to calculate polymer stress from simulated polymer dynamics [9]. Combination of microscopic models with stochastic simulation techniques eliminates the need of traditional closed form model and provides a direct link between the flow process and the micro-structure of the fluid. In addition, improvements of the model can be made in molecular level within the framework of stochastic processes.

In 1998 Feigl and Öttinger [3], introduced a class of stochastic models which combines the aspects of macroscopic models with aspects of reptation and network models. Feigl and Senaratne [4] developed a micro-macro algorithm incorporating a stochastic model from the same class to calculate the die-entry flow of a polymeric fluid. The purpose of this paper is to develop the stochastic model discussed in Feigl and Senaratne [4] by considering non-affine motion of the configurations of macromolecules. The model is evaluated by computing its predictions to various material functions of a polymeric fluid in simple rheometric flows. The simulation results are compared with available experimental data of Quinzani et al. [11], [12].

2. Model Description

The dynamics of the model are two independent Gaussian stochastic processes which describe the configurations of temporary physical entanglements of the macromolecules in the fluid. These configuration vectors, $\boldsymbol{Q}_1(t)$ and $\boldsymbol{Q}_2(t)$, are randomly generated, allowed to evolve according to deterministic equations during their respective lifetimes, destroyed, and independently regenerated. During their lifetimes s_1 and s_2, these vectors evolve according to the equations of motion

$$\frac{d\boldsymbol{Q}_1(t)}{dt} = \left(\boldsymbol{\kappa} - \tilde{\boldsymbol{\kappa}}\right)\cdot\boldsymbol{Q}_1(t) \qquad t' < t < t' + s_1 \tag{3}$$

$$\frac{d\boldsymbol{Q}_2(t)}{dt} = -\left(\boldsymbol{\kappa}^{\dagger} + \tilde{\boldsymbol{\kappa}}\right)\cdot\boldsymbol{Q}_2(t) \qquad t' < t < t' + s_2 \tag{4}$$

where t' is the creation time of the vectors, $\tilde{\boldsymbol{\kappa}}$ is the slip tensor given by $\tilde{\boldsymbol{\kappa}}(t) = a\dot{\boldsymbol{\gamma}}/2$, $\dot{\boldsymbol{\gamma}}$ is the velocity gradient tensor, and a is the slip parameter. The slip tensor accounts for the non-affine

motion of the configuration vectors $\boldsymbol{Q}_1(t)$ and $\boldsymbol{Q}_2(t)$ in the flow field. At time $t = t' = 0,$ each vector is an independent Gaussian process with mean $\left\langle \boldsymbol{Q}_i\left(t'\right)\right\rangle = 0$ and covariance $\left\langle \boldsymbol{Q}_i\left(t'\right), \boldsymbol{Q}_i\left(t'\right)\right\rangle = \boldsymbol{\delta}, \quad i = 1,2,$ where $\boldsymbol{\delta}$ is the 3×3 unit tensor. At the time $t = t' + s_i, \quad i = 1,2,$ the vector $\boldsymbol{Q}_i(t), i = 1,2,$ is destroyed and independently regenerated according to the standard Gaussian distribution.

The vector $\boldsymbol{Q}_1(t)$ represents the end-to-end dimensionless configuration vector from network theory for concentrated polymer melts and polymer solutions as described by Bird et al. [1]. It describes the configurations of the segments or tubes that define the temporary physical entanglements of the macromolecules in the temporary network. At time t' the segment is created and it evolves according to Eq. (3) during its lifetime s_1. The segment is destroyed and independently regenerated according to the standard Gaussian distribution at time $t = t' + s_1.$ The vector $\boldsymbol{Q}_2(t)$ represents the anisotropic tube cross section of reptation theory described by **Öttinger** [8] – [10]. It describes the reptation motion of the polymer, which is restricted to a tube formed by the surrounding macromolecules. The vector $\boldsymbol{Q}_2(t)$ points from the centerline of the tube to the wall of the tube. Its equation of motion, Eq. (4), describes the change of the tube diameter during its life time s_2.

The life time $s_i, i = 1,2,$ of each vector is determined form a probability density function $p(s)$, which is related to the fluid's memory function, $m\left(t - t'\right)$, via

$$\frac{m\left(t - t'\right)}{m(0)} = \int_{t-t'}^{\infty} p(s)ds. \tag{5}$$

Once the memory function for the material is determined, a coordinate transformation between a random number $z \in [0,1)$ and $s_i, i = 1,2,$ can be used to obtain a more convenient expression for $s_i, i = 1,2,$ is given by

$$z(s) = \int_0^s p\left(s'\right)ds' = 1 - \frac{m(s)}{m(0)} \tag{6}$$

where $s = t - t'.$ As z ranges from 0 to $1,$ s increase monotonically from 0 to ∞.

In general, the memory function is taken to be the Maxwell's linear visco-elastic memory function, which is given by

$$m(s) = \sum_{k=1}^{K} \frac{\eta_k}{\lambda_k} e^{-s/\lambda_k} \tag{7}$$

where, $\{\lambda_k, \eta_k\}$, $k = 1, \cdots, K$ are a set of relaxation times and partial viscosities for the material. The relaxation spectrum can be found by fitting Eq. (7) to linear visco-elastic data of the fluid.

3. Stress Tensor

Given a stochastic rheological model, the dimensionless polymer contribution to the extra stress tensor $\boldsymbol{\tau}_p$ is expressed as an expectation of a function $\boldsymbol{F}$ which involves the dynamics of the model. As described by Feigl et al. [3], we take $\boldsymbol{\tau}_p$ to be

$$\boldsymbol{\tau}_p(t) = G(0)\left\langle \boldsymbol{F}\left(\boldsymbol{Q}(t)\right)\right\rangle \tag{8}$$

$$\left\langle \boldsymbol{F}\left(\boldsymbol{Q}(t)\right)\right\rangle = \left\langle f_1 \boldsymbol{Q}_1(t)\boldsymbol{Q}_1(t) + f_2 \boldsymbol{Q}_2(t)\boldsymbol{Q}_2(t)\right\rangle \tag{9}$$

where $G(0)$ is the value of the relaxation modulus, $G(t-t')$, at $t = t'$ and $f_1 = f_1\left(Q_1^2, Q_2^2\right)$ and $f_2 = f_2\left(Q_1^2, Q_2^2\right)$ are scalar functions of $Q_i^2 = tr\,\boldsymbol{Q}_i\,\boldsymbol{Q}_i$, $i = 1, 2$. These functions are similar to the strain functions in the factorized Rivlin Sawyers model described by Rivlin et al. [13] and hence represent the continuum part of the model. The parameters contain in these functions can be chosen to fit rheological data of the material in concern.

Finally, in order to ensure that the correct linear viscoelastic behavior is described by the model, the functions f_1 and f_2 must satisfy the constraint

$$\frac{\eta_p}{\eta_p + \eta_s} = \frac{1}{3}\left\langle Q_1^{e2} f_1^e - Q_2^{e2} f_2^e \right\rangle_0 + \frac{2}{15}\left\langle \left(Q_1^{e2}\right)^2 f_{1,1}^e - \left(Q_2^{e2}\right)^2 f_{2,2}^e \right\rangle_0 \tag{10}$$

where η_p is the polymer contribution to the zero shear rate viscosity $\eta_0 = \eta_p + \eta_s$ and $\langle . \rangle_0$ indicates taking a Gaussian average in six-dimensional space with respect to the Gaussian probability density in six-dimensional space with mean 0 and square of the width δ.

Furthermore, $Q_i^e = Q_i(0)$ denotes the value of Q_i at equilibrium, and we adopt the notation $f_i^e = f_i\left(Q_1^{e2}, Q_2^{e2}\right), i = 1,2$ and $f_{i,j}^e = \frac{\partial f_i}{\partial Q_j^2}\left(Q_1^{e2}, Q_2^{e2}\right), \quad i, j = 1,2.$ This constraint is derived by assuming that a fluid which is at equilibrium at time $t = 0$ undergoes a small shear deformation. The details of the derivation are given in Feigl et al. [3].

4. Simulation algorithm

The general simulation procedure to compute polymer stress for a given fluid in homogeneous flow can be briefly described as follows. Consider two independent ensembles, $\left\{\boldsymbol{Q}_1^k(t)\right\}_{k=1}^{N_T}$ and $\left\{\boldsymbol{Q}_2^k(t)\right\}_{k=1}^{N_T}$ for the random variables $\boldsymbol{Q}_1(t)$ and $\boldsymbol{Q}_2(t)$, where N_T is the size of the ensembles. Let $t = T$, be the time at which the polymer stress, $\boldsymbol{\tau}_p$, is to be computed. Divide the time interval $[0,T]$ into M subintervals $\left[t_{j-1}, t_j\right]$, $j = 1,\cdots,M$. Then, repeat the following steps for $k = 1,\cdots,N_T$ until the time T is reached.

1. Randomly generate $\boldsymbol{Q}_i^k$ from a standard Gaussian distribution with mean zero and covariance $\boldsymbol{\delta}$, for $i = 1, 2.$

2. Randomly generate a survival time s_i^k for $\boldsymbol{Q}_i^k, i = 1,2,$ from a given probability density $p(s)$ which corresponds to a given relaxation spectrum, or memory function $m\left(t - t'\right)$.

3. Evolve $\boldsymbol{Q}_i^k$ according to the corresponding equation of motion for the duration of the survival time s_i^k for $i = 1, 2$. The first-order explicit Euler method is applied to numerically integrate the Eq.(3) and Eq.(4) during the lifetime of each vector $\boldsymbol{Q}_i^k$, $i = 1,2,$ $k = 1,\cdots N_T$.

When time $t = T$ is reached calculate polymer stress $\boldsymbol{\tau}_p$ by substituting values of $\boldsymbol{Q}_1^k$ and $\boldsymbol{Q}_2^k$ into Eq.(9) for each k and average over all k to obtain the dimensionless polymer stress $\boldsymbol{\tau}_p$.

In step two of the above algorithm, the lifetime s_i^k has to be generated for each ensemble $\boldsymbol{Q}_i^k$ from the probability density function $p(s)$ of survival time using Eq. (6). The expression for

$z = z(s)$ in Eq.(6) cannot be conveniently inverted to produce an analytical expression for $s = s(z)$ for a multi-mode memory function ($k > 1$). However, since the Maxwell's memory function in Eq. (7) is used, for each mode k, the expression for $z(s)$ can be analytically solved for s. From Eq.(5) the probability density associated with Eq.(7) becomes

$$p(s) = \frac{1}{m(s)} \sum_{k=1}^{K} \frac{\eta_k}{\lambda_k^3} e^{-s/\lambda_k} \tag{11}$$

For each single mode k Eq.(6) reduces to

$$z(s) = 1 - exp\left(-s/\lambda_k\right) \tag{12}$$

From which

$$s(z) = -\lambda_k \, ln(1-z) \tag{13}$$

can be obtained. Since the multi mode model can be expressed as a sum of single-mode models, each mode is simulated separately according to the given algorithm until time $t = T$ is reached. Once time $t = T$ is reached, the polymer stress corresponding to the relaxation time λ_k is computed and the results are averaged over all relaxation times to obtain $\boldsymbol{\tau}_p(T)$.

When a memory function of the form in Eq. (7) is known, single mode simulation is shown to be the more accurate, robust and flexible method. However, if there are a larger number of modes in the relaxation spectrum of the fluid in concern, this single simulation approach is less attractive due to the increased computational time. In this case, one lifetime can be generated from the entire spectrum using nonlinear iteration scheme to solve Eq. (6). We use single mode simulation approach for all simulations in this paper since the fluid under consideration has a small spectrum.

For each mode k, time is non-dimensionalized in the simulation by the relaxation time, λ_k, and the computed non-dimensional stress contribution from this mode is multiplied by η_k / λ_k to get the dimensional stress contribution for the mode k. The results are accumulated over sum of all modes.

From Eq. (6), the $ij-$ component of the polymer contribution to the stress tensor, $\boldsymbol{\tau}_p$ at time t is given by

$$\tau_{ij}^{p}(t) = G(0)\left\langle F_{ij}\left(\boldsymbol{Q}_1(t), \boldsymbol{Q}_2(t)\right)\right\rangle. \tag{14}$$

The mean of the random variable in the right hand side of Eq. (14) is approximated by the ensemble average determined by taking the arithmetic mean of F_{ij} over realizations as follows

$$\left\langle F_{ij}\left(\boldsymbol{Q}_1(t),\boldsymbol{Q}_2(t)\right)\right\rangle \cong \frac{1}{N_T}\sum_{k=1}^{N_T} F_{ij}\left(\boldsymbol{Q}^k(t)\right). \tag{15}$$

The statistical error for the ensemble is defined to be

$$e_{stat} = \sqrt{\frac{var\left[F_{ij}(\boldsymbol{Q}(t))\right]}{N_T}} \tag{16}$$

where the variance is given by

$$var\left[F_{ij}(\boldsymbol{Q}(t))\right] = \left\langle F_{ij}\left(\boldsymbol{Q}(t)\right)^2\right\rangle - \left\langle F_{ij}\left(\boldsymbol{Q}(t)\right)\right\rangle^2. \tag{17}$$

4.1 Variance reduction

The statistical errors of the simulations can be reduced by increasing the size of the ensemble, N_T, or by decreasing the variance of the quantity of interest $F_{ij}\left(\boldsymbol{Q}(t)\right)$. It has been shown that for a given ensemble N_T, the statistical error increases for small deformations and increasing the ensemble size N_T has little effect on the error. On the other hand, variance reduction techniques that reduce the statistical error for the same ensemble size have been very efficient and powerful for stochastic simulations. The basic idea of variance reduction techniques is to construct an estimator for the desired average which has the same mean, but a smaller variance. This in turn will lead to a smaller statistical error for the same ensemble size.

For all the results presented in this paper, a variance reduction technique based on equilibrium control variates as described by Melchior et al. [7] has been used to reduce statistical errors. This method allows one to seize the fluctuations of the quantity of interest, here $F_{ij}\left(\boldsymbol{Q}(t)\right)$ around its mean. The fluctuation of $F_{ij}\left(\boldsymbol{Q}(t)\right)$ around its mean is given by $C_t = F_{ij}\left(\boldsymbol{Q}(t)\right) - \left\langle F_{ij}\left(\boldsymbol{Q}(t)\right)\right\rangle$. Since the exact form of fluctuations is not known, it is necessary to construct a control variate $\hat{E}(t) = F_{ij}\left(\boldsymbol{Q}(t)\right) - \hat{C}(t)$ to be used as an unbiased estimator for $F_{ij}\left(\boldsymbol{Q}(t)\right)$ whose variance can be reduced with a good choice of control variable $\hat{C}(t)$. The approximation for $\hat{C}(t)$ should be chosen to have mean zero and reduce the variance of $\hat{E}(t)$.

In other words $\hat{C}(t)$ should satisfies $\left\langle \hat{E}(t) \right\rangle = \left\langle F_{ij}\left(\boldsymbol{Q}(t)\right) \right\rangle$ and $Var\left(\hat{E}(t)\right) < Var\left[F_{ij}\left(\boldsymbol{Q}(t)\right) \right]$. One choice of approximation is $\hat{C}(t) = F_{ij}\left(\tilde{\boldsymbol{Q}}(t)\right) - \left\langle F_{ij}\left(\tilde{\boldsymbol{Q}}(t)\right) \right\rangle$, where $\tilde{\boldsymbol{Q}}(t)$ is a stochastic process which approximates the true dynamics $\boldsymbol{Q}(t)$ of the model. With approximate dynamics, $\tilde{\boldsymbol{Q}}(t)$ taken to be those of equilibrium, variance reduction is achieved through parallel process simulation in which two simulations are simultaneously performed using trajectories constructed from the same sequence of the random numbers. One simulation uses the true dynamics while the other simulation uses the approximate dynamics and the results are then subtracted to achieve reduce variance.

5. Material description and model predictions of material functions

The performance of the stochastic model is evaluated by computing material functions of a polymeric fluid and making comparisons with available experimental data, and with the known qualitative behavior of the fluid. The fluid considered was a concentrated polymer solution, a 5% polyisobutylene (PIB) solution in tetradecane (c14) at $25℃$ described by Quinzani et al. [11]-[12].

The microscopic-based stochastic model is defined by the linear visco-elastic relaxation spectrum $\{a_k, \lambda_k\}$, strain functions f_1 and f_2, and the slip parameter a. The relaxation spectrum for the PIB solution was determined by Quinzani et al. [12] and is given in Table 1.

Table 1: Relaxation Spectrum of the PIB Solution.

Mode Number	λ_i [$Pa\ s$]	η_i [$Pa\ s$]
1	0.6855	0.0400
2	0.1396	0.2324
3	0.0389	0.5644
4	0.0059	0.5850

The extra stress tensor $\boldsymbol{\tau}$ for the PIB solution is expressed in terms of polymer contribution $\boldsymbol{\tau}_p$ and a small Newtonian solvent contribution $\boldsymbol{\tau}_s$ as $\boldsymbol{\tau} = \boldsymbol{\tau}_p + \boldsymbol{\tau}_s$. Similarly, the zero-shear-rate viscosity η_0 of the fluid is expressed as $\eta_0 = \eta_p + \eta_s$ where η_s is the solvent viscosity and η_p is the polymer viscosity. According to the calculations in Quinzani et al. [11, 12], $\eta_0 = 1.4258\ Pa\ s$, $\eta_p = 1.4238\ Pa\ s$, and $\eta_s = 0.002 Pa\ s$.

Feigl and Senaratne [4] previously derived a model of the form in Eq. (9) for the PIB solution. For the model discussed here, we use the same strain functions which are given by

$$f_1\left(Q_1^2, Q_2^2\right) = \frac{1}{a_0 + a_1 Q_1^2 + a_2 Q_2^2}, \quad f_2 = 0 \tag{18}$$

where $a_0 = 0.635, a_1 = 0.040, a_2 = 0.038$ are the parameters. The slip parameter a is taken to be 0.18. These parameters are chosen to satisfy the small deformation constraint and to satisfy the linear visco-elastic behavior of the PIB solution.

The material functions of the PIB solution are computed in the steady shear flow, start-up of steady shear flow and steady elongational flow. The steady state material functions are calculated by using the principle of ergodicity. In this approach a single trajectory is tracked for the simulation time T which is taken to be large enough to reach the steady state. For the calculation of transient material functions, an ensemble of $N_T = 10^7$ trajectories was used for each ensemble. For both cases vectorization was employed to reduce the computational time.

5.1 Steady Shear flow

The steady shear flow is defined by the vector field

$$v_x = \dot{\gamma}_{21}, \quad v_y = 0, \quad v_z = 0 \tag{19}$$

where the shear rate, $\dot{\gamma}_{21} = \dot{\gamma}$, is a constant. The computed material functions are shear viscosity, first normal stress coefficient, the second normal stress coefficient, respectively given by

$$\eta = \frac{\tau_{12}}{\dot{\gamma}}, \quad \psi_1 = \frac{\tau_{11} - \tau_{22}}{\dot{\gamma}^2}, \quad \psi_2 = \frac{\tau_{22} - \tau_{33}}{\dot{\gamma}^2} \tag{20}$$

and the normal stress ratio $-\psi_2/\psi_1$.

Fig. 1 shows the model's predictions of the shear viscosity, η, and the first normal stress coefficient, ψ_1, as a function of shear rate $\dot{\gamma}$ and experimental data for the PIB solution. The horizontal dash lines represent the zero shear rate viscosity $\eta_0 = \eta_p + \eta_s = 1.4258\ Pa\,s$ and the zero shear rate first normal stress coefficient computed from the generalized Maxwell's model. The experimental data were read from graphs of Quinzani et al. [12] for various temperatures and shifted to a master curve at $25°C$ via time-temperature superposition. The statistical error bars of these simulations are not visible since they were very small compared to the size of the symbols. This is the case for all Fig.s presented in this paper. The model predicts very well the shear viscosity and the first normal stress difference both qualitatively and quantitatively.

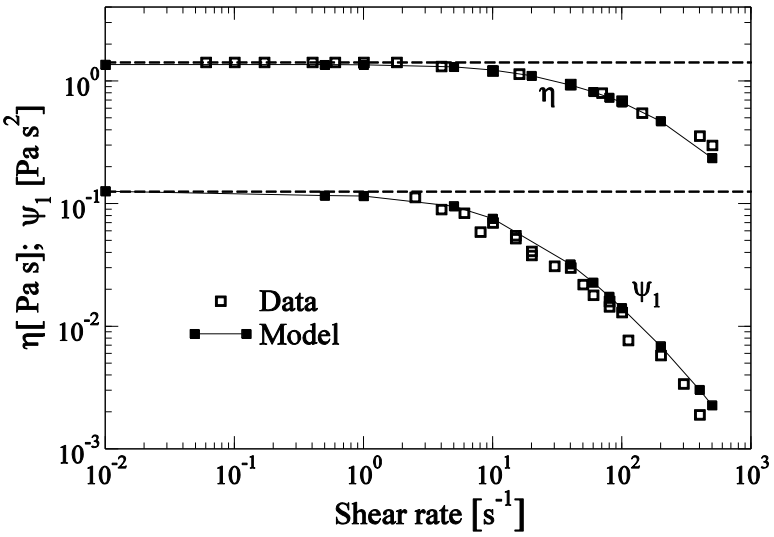

Fig. 1: Model predictions of shear viscosity and the first normal stress coefficient in steady shear flow and comparisons to experimental data. The dashed horizontal lines represent the zero-shear-rate viscosity and the first normal stress coefficient.

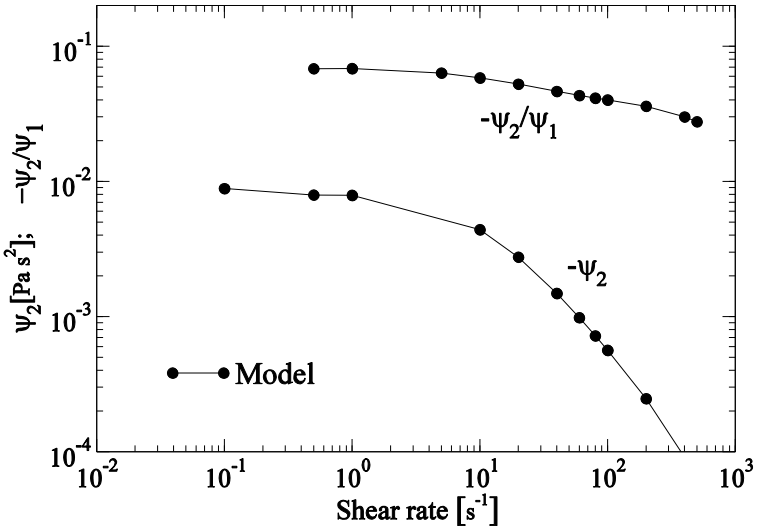

Fig. 2: Model Predictions Of Second Normal Stress Coefficient And The Normal Stress Ratio For The PIB Solution In Steady Shear Flow.

Model's predictions for the second normal stress coefficient, ψ_2, and the nonzero normal stress ratio, $-\psi_2/\psi_1$, in simple steady shear flow are given in Fig. 2 although no experimental data is available for comparison. The model correctly predicts the standard non-zero second normal stress coefficient, ψ_2, and a decrease in the normal stress ratio with increased shear rate $\dot{\gamma}$. There are very few experimental data on second normal stress coefficient, ψ_2, and the normal stress ratio, $-\psi_2/\psi_1$, of polymeric fluids. The limited experimental data shown in Bird et al.[1] and Morrison [6], indicate that for a concentrated polymer solution the values of the normal stress ratio are in the range of $0.01-0.20$. The graph shows that the values predicted by the model lie in this range.

5.2. Startup of Steady Shear Flow

Shear viscosity and the first normal stress coefficient are of particular interest in the startup flow of polymeric fluids. The velocity profile for the startup of steady shear flow is given by Eq. (19), where the shear rate is given by $\dot{\gamma}_{21} = 0$ for $t < 0$ and $\dot{\gamma}_{21} = \dot{\gamma}_0$ for $t > 0$, where $\dot{\gamma}_0$ is a constant. The fluid was simulated for a wide range of shear rates ranging from 0.1 to 100 and model's predictions were compared with experimental data. An example of this comparison for two shear rates is given in Fig. 3. Comparisons of the model's predictions to shear viscosity

η^+ with experimental data showed that the model predicts the transient shear viscosity well for all shear rates considered including the small overshoot at $\dot{\gamma} = 100\, s^{-1}$. This overshoot before reaching steady state is typical for polymeric fluids at higher shear rates.

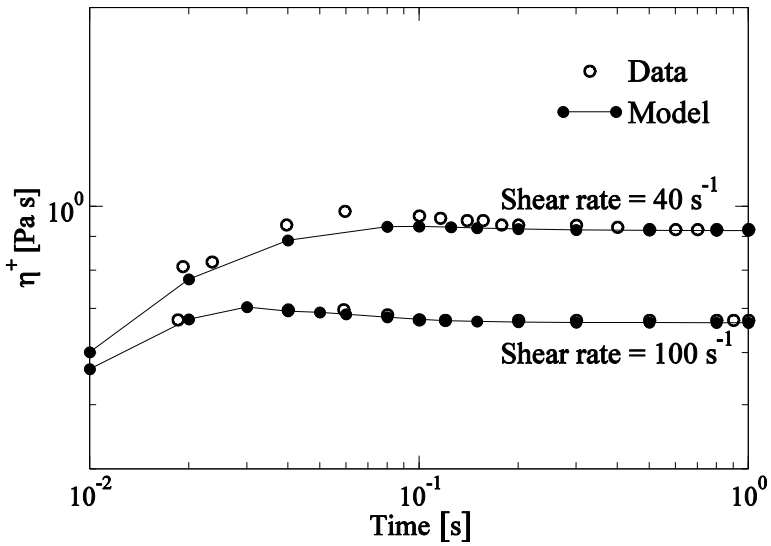

Fig. 3: Model Predictions Of Viscosity In Startup Of Shear Flow For The PIB Solution And Comparison To Experimental Data.

The simulation results for the first normal stress coefficient, ψ_1^+, along with experimental data are shown in Fig. 4. Although model captures the correct qualitative behavior, it does not capture the apparent overshoot seen in the experimental data. This discrepancy was observed for all the shear rates considered.

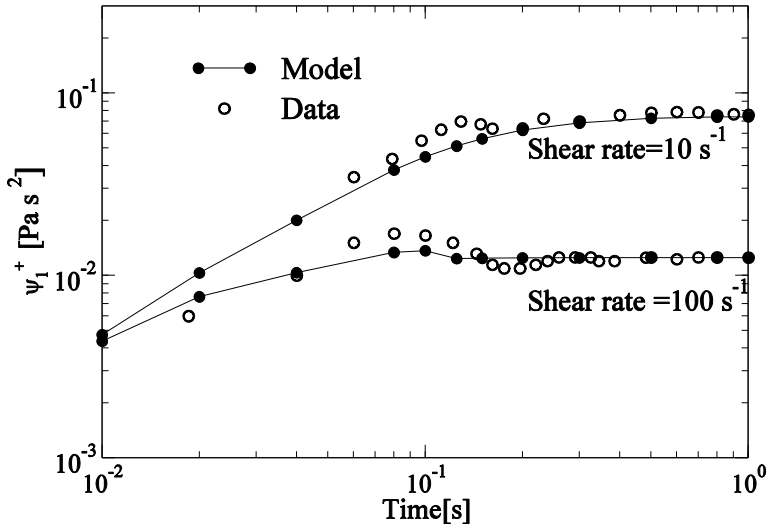

Fig. 4: Model Predictions Of First Normal Stress Coefficient For The PIB Solution In Startup Of Shear Flow And Comparisons To Experimental Data.

5.3 Steady Elongational Flow

The steady uniaxial elongational flow is defined by the velocity field

$$v_x = -\dot{\varepsilon}\, x/2, \quad v_y = -\dot{\varepsilon}\, y/2, \quad v_z = \dot{\varepsilon} z$$

where $\dot{\varepsilon}$ is the applied elongational rate and $\dot{\varepsilon} > 0.$ The uniaxial elongational viscosity, $\bar{\eta},$ is defined by

$$\bar{\eta} = -\frac{\tau_{33} - \tau_{11}}{\dot{\varepsilon}}.$$

Fig. 5 show that the model predicts the correct qualitative behavior of elongational viscosity $\bar{\eta}$ in steady elongational flow. The dashed horizontal line represents the trouton viscosity, $3\eta_0$, which is three times the zero-shear-rate viscosity. For many polymers, the zero-shear-rate elongational viscosity $\bar{\eta}_0$ is same as the Trouton viscosity and model correctly predicts this qualitative behavior for the PIB solution. The graph also indicates the correct qualitative behavior of strain-hardening for the elongation viscosity, $\bar{\eta}$. Reliable experimental data for elongational viscosity $\bar{\eta}$ are not available for a comparison.

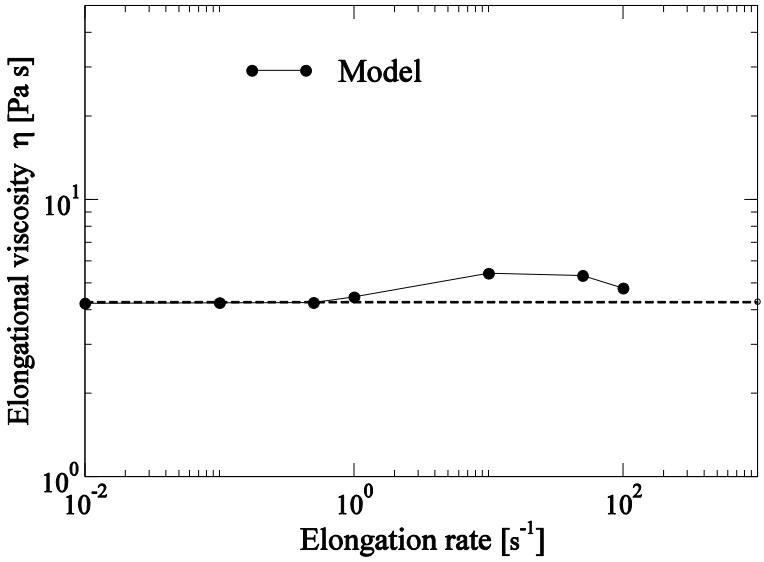

Fig. 5: Model Predictions Of Steady Uniaxial Elongational Viscosity For The PIB Solution In Steady Elongational Flow.

6. Summary and Conclusions

A microscopic based stochastic rheological model for the calculation of polymeric stress was described and evaluated. The model describes the macromolecules of the fluid and their evolution with the flow field. The dynamics of the macromolecules, which are originated from network theory and reptation theory, are modeled by two stochastic processes which represent the configuration vectors of the macromolecules, together with the survival times of these processes. The survival time for each process is randomly generated from a probability density determined from the material's relaxation spectrum. The aspects of macroscopic models are built into the model through the strain functions f_1 and f_2, thus the model considered here offers a blending of macroscopic and microscopic models.

The model was evaluated by simulating the flow of a concentrated PIB solution in various rheometrc flows and computing material functions and comparing them with available experimental data reported by Quinzani et al. [11, 12]. The specific form of the model for the PIB solution was derived by making the second strain function to be identically zero. The slip parameter and the other parameters in the strain functions are chosen to satisfy the linear visco-elastic behavior of the material.

The model accurately predicts the shear viscosity and the first normal stress coefficient in simple steady shear flow for a range of shear rates. It also correctly predicts the non-zero second

normal stress difference which remains negative. The predictions of the magnitude of the normal stress ratio are reasonable. In the startup of steady shear flow the model predictions of η^+ agree very well with the experimental data. Although the predictions for ψ_1^+ agree generally well with the experimental data, the model does not capture the overshoot shown in the experimental data. Finally, the model predicts the correct qualitative behavior for the steady elongational viscosity. The model can be further improved by making modifications to the model dynamics $\boldsymbol{Q}_1(t)$ and $\boldsymbol{Q}_2(t)$. This can be achieved through the inclusion of a restoring force or noise to the deterministic equations of motion.

References

[1] R.B. Bird, C.F. Curtiss, R.C. Armstrong, O. Hassager, "Dynamics of Polymeric Liquids," Wiley-Interscience, New York, vol. 2, 1987.

[2] M. Doi, S.F. Edwards, "The theory of Polymer Dynamics," Oxford University Press, Oxford, 1986.

[3] K. Feigl, H.C. Öttinger , "A new class of stochastic simulation models for polymer stress calculation," J. Chemical Physics, vol. 109, 1998, pp. 815-826.

[4] K. Feigl, D.C. Senaratne, "Calculation of the die entry flow of a concentrated polymer solution using micro-macro simulations," J. Fluid. Eng., vol. 128, 2006, pp. 55-61.

[5] K. Feigl, H.C. Öttinger , "The equivalence of the class of Rivlin-Sawyers equations and a class of stochastic models for polymer stress," J. Math. Phys. vol. 42, 2001, pp. 796-817.

[6] F.A. Morrison, "Understanding Rheology," Oxford University Press, New York, 2001.

[7] Melchior M., H.C. Öttinger , "Variance reduced simulations of polymer dynamics", J. Chem. Phys., vol. 105, 1996, pp. 3316-3330.

[8] H.C.Öttinger , "Computer simulation of Reptation theories. Doi-Edwards and Curtiss-Bird models," J. Chemical Physics, vol. 91, 1989, pp. 6455-6462.

[9] H.C. Öttinger , "Stochastic Processes in Polymeric Fluids," Springer, Berlin, 1996.

[10] H.C. Öttinger , "Thermo dynamically admissible reptation models with anisotropic tube cross sections convective constraint release," J. Non-Newtonian Fluid Mech., vol. 89, 2000, pp. 165-185.

[11] L.M. Quinzani, G.H. McKinley, R.A. Brown, R.C. Armstrong, "Modeling the rheology of polyisobutylene solutions," J. Rheology, vol. 34, 1990, pp.705-748.

[12] L.M. Quinzani, R.C Armstrong, R.A.Brown, "Use of Coupled birefringence and LDV studies of flow through a planar contraction to test constitutive equations for concentrated polymer solutions," J. Rheology, vol.6, 1995, pp. 1201-1228.

[13] R.S.Rivlin, K.N.Sawyers, "Nonlinear mechanics of visco elastic fluids," Ann. Rev. Fluid Mech., vol. 3, 1971, pp. 117-146.